Data, Innovation, and Science Cluster

Swarm-PRISM Description of the Processing Algorithm

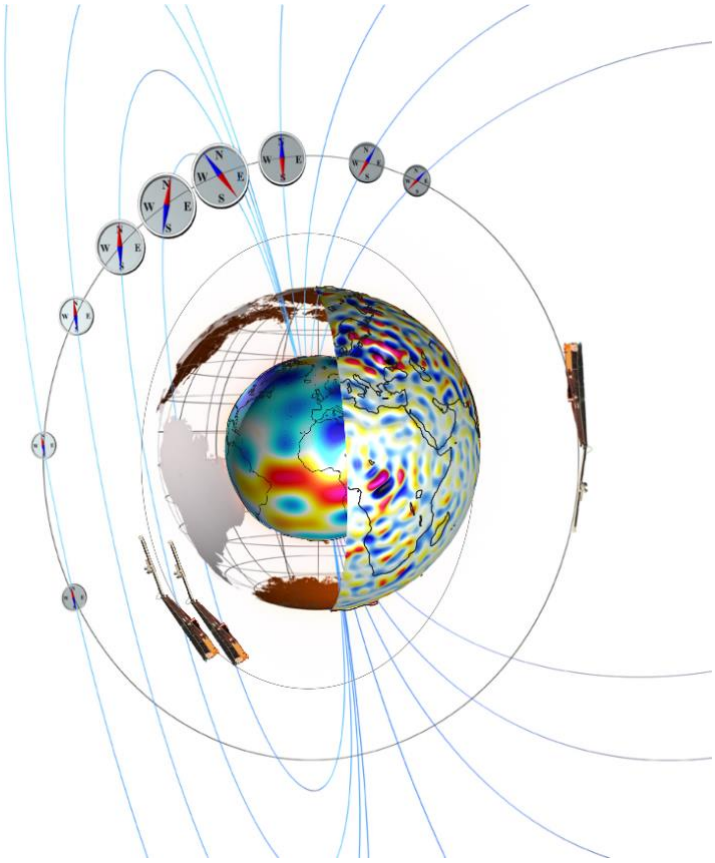

Doc. no: SW-DS-GFZ-GS-006, Rev: 2, 25 Jun 2021

Prepared:

Balazs Heilig Date 25 Jun 2021

Scientist

Approved: Claudia Stolle

Digitally signed by Claudia Stolle
Date: 2021.06.28 16:28:55 +02'00'

Claudia Stolle Date 25 Jun 2021

Team Leader

Checked: Guram Kervalishvili

DN: cn=Guram Kervalishvili, o=GFZ German Research Centre for Geosciences, email=gmk@gfz-potsdam.de, c=DE
Date: 2021.06.28 15:21:57 +02'00'

Guram Kervalishvili Date 25 Jun 2021

Scientist

Record of Changes

Reason	Description	Rev	Date
Initial vers.	Released.	1 dA	23 Apr 2020
Updated in response to DISC comments	Document text has been updated and corrected with minor changes. Figure 4-2, Figure 4-3, and Figure 4-5 have been updated.	1 dB	26 May 2020
Updated input from GFZ	Sections 4.1.3, 4.3.4, 4.5.3, and Figure 4-8 have been updated.	1 dC	29 May 2020
Updated input from GFZ	Minor text updates in some parts of the text. Sections 4.1.2.3, 4.1.2.4, 4.1.2.5, 4.1.2.6, 4.1.2.7 and 4.1.2.8 have been updated. New sections 4.1.2.9, 4.2, 4.4 and 4.6 have been added.	1 dD	12 Mar 2021
Signature		1	18 Mar 2021
Email from Klaus to Guram: 09.06.2021 10h05	Figure 4-2, Figure 4-5 and text updates according to reviewers' comments.	2 dA	24 Jun 2021
Signature		2	25 Jun 2021

Table of Contents

List of Figures

List of Tables

1 Introduction

1.1 Scope and applicability

This document comprises the description of the processing algorithms of the Swarm Level 2 (L2) PRISM products in response to the requirements of [AD-1]. Swarm PRISM includes the following three products [AD-2]:

- **MITx_LP_2F** – Characterisation of the **M**id-latitude **I**onospheric **T**rough based on Langmuir probe observations
- **MITxTEC_2F** – Characterisation of the **M**id-latitude **I**onospheric **T**rough based on GNSS TEC observations
- **PPIxFAC_2F** – Midnight **P**lasma**P**ause **I**ndex and equatorward boundary of small-scale field aligned currents

The Swarm-PRISM Product Definition document [AD-2] is available in the SVN folder: https://smart-svn.spacecenter.dk/svn/smart/SwarmDISC/DISC_Projects/ITT2_2_PRISM/Deliverables/.

Current or updated version of this document is available in the SVN folder: https://smart-svn.spacecenter.dk/svn/smart/SwarmDISC/DISC_Projects/ITT2_2_PRISM/Deliverables/.

2 Applicable and Reference Documentation

2.1 Applicable Documents

The following documents are applicable to the definitions within this document.

[AD-1] SW-OF-GFZ-GS-122_2-2_PRISM_Proposal, Proposal for Swarm DISC ITT 2.2, Swarm-PRISM – Plasmapause Related boundaries in the topside Ionosphere as derived from Swarm Measurements.

[AD-2] TN-01: SW-DS-GFZ-GS-003_2-2_PRISM_PDD, Product Definition Document.

[AD-3] TN-02: SW-DS-GFZ-GS-004_2-2_PRISM_Work-plan, Work plan.

[AD-4] SW-RS-DSC-SY-0007, Swarm Level 1b Product Definition.

2.2 Reference Documents

The following documents contain supporting and background information to be taken into account during the activities specified within this document.

[RD-1] Heilig, B. and Lühr, H. (2013), New plasmapause model derived from CHAMP field-aligned current signatures, Ann. Geophys., 31, 529-539, doi: 10.5194/angeo-31-529-2013.

[RD-2] Heilig, B. and Lühr, H. (2018), Quantifying the relationship between the plasmapause and the inner boundary of small-scale field-aligned currents, as deduced from Swarm observations, Ann. Geophys. 36, 595-607, doi: 10.5194/angeo-36-595-2018.

[RD-3] Prölss, G. W. (2007), The equatorward wall of the subauroral trough in the after-noon/evening sector, Ann. Geophys., 25, 645–659, doi: 10.5194/angeo-25-645-2007.

[RD-4] Matyjasiak, M., D. Przepiórka, and H. Rothkaehl (2016), Seasonal Variations of Mid-Latitude Ionospheric Trough Structure Observed with DEMETER and COSMIC, Acta Geophysica, 64(6), 2734-2747, doi: 10.1515/acgeo-2016-0102.

[RD-5] Prölss, G. W. (2006), Subauroral electron temperature enhancement in the nighttime ionosphere, Ann. Geophys., 24, 1871-1885, doi: 10.5194/angeo-24-1871-2006.

[RD-6] Pedatella, N. M. and Larson, K. M. (2010), Routine determination of the plasmapause based on COSMIC GPS total electron content observations of the midlatitude trough, J. Geophys. Res., 115, A09301, doi: 10.1029/2010JA015265.

[RD-7] Yang, N., H. Le, and L. Liu (2015), Statistical analysis of ionospheric mid-latitude trough over the Northern Hemisphere derived from GPS total electron content data, Earth, Planets and Space, 67:196, doi: 10.1186/s40623-015-0365-1.

[RD-8] Horvath, I., and B. C. Lovell (2009), Investigating the relationships among the South Atlantic Magnetic Anomaly, southern nighttime midlatitude trough, and nighttime Weddell Sea Anomaly during southern summer, J. Geophys. Res., 114, A02306, doi: 10.1029/2008JA013719.

[RD-9] Yizengaw, E., Wei, H., Moldwin, M. B., Galvan, D., Mandrake, L., Mannucci, A. and Pi, X. (2005), The correlation between mid-latitude trough and the plasmapause, Geophys. Res. Lett., 32, L10102, doi: 10.1029/2005GL022954.

[RD-10] Chen, C. Y., Liu, T. J. Y., Lee, I. T., Rothkaehl, H., Przepiorka, D., Chang, L. C., et al. (2018), The midlatitude trough and the plasmapause in the nighttime ionosphere simultaneously observed by DEMETER during 2006–2009, Journal of Geophysical Research: Space Physics, 123, doi: 10.1029/2017JA024840.

[RD-11] Heilig, B., C. Stolle, G. Kervalishvili, J. Rauberg, Y. Miyoshi, F. Tsuchiya, A. Kumamoto, Y. Kasahara, M. Shoji, S. Nakamura, M. Kitahara, I. Shinohara (2021), Relation between the Plasma-pause Dynamics and the Mid-latitude Ionospheric Trough as Observed in the Topside Ionosphere by Swarm, submitted to Journal of Geophysical Research: Space Physics.

2.3 Abbreviations

A list of acronyms and abbreviations used by Swarm partners can be found here. Any acronyms or abbreviations not found on the online list but used in this document can be found below.

Acronym ***or abbreviation***	***Description***
E-field	Electric field
EW	EquatorWard
IGRF	International Geomagnetic Reference Field
L-value	The McIlwain L-parameter, distance of the field line apex from the centre of the Earth measured in Earth radii
LP	Langmuir Probe
MIT	Mid-latitude Ionospheric Trough

Acronym ***or abbreviation***	***Description***
Ne	electron number density
PP	PlasmaPause
PRISM	Plasmapause Related boundaries in the topside Ionosphere as derived from Swarm Measurements (this project)
PW	PoleWard
QD	Quasi-Dipole
SAID	Sub-Auroral Ion Drift
SAPS	Sub-Auroral Polarisation Stream
SETE	Sub-auroral Electron Temperature Enhancement
SSFAC	Small-Scale FAC
Te	electron temperature

3 Scientific and Technical Background

3.1 The Mid-latitude Ionospheric Trough and its relation to the Plasmapause

The Swarm-PRISM products [AD-2] contribute to the monitoring of physical processes taking place in the sub-auroral ionosphere. As a consequence of the magnetosphere-ionosphere coupling, and especially the coupling between sub-auroral processes and the dynamics of the plasmaspheric boundary layer, all PRISM products carry also information on plasmasphere dynamics. The following background information where no specific reference is given comes from [RD-11].

The MIT appears as a few-degree-wide depleted zone in the nighttime sub-auroral ionosphere. MIT is often associated with the plasma flow stagnation zone near dusk where the corotation and the convection E-fields counteract each other. The depletion is believed to propagate to later local times as a result of corotation. The MIT is typically found immediately equatorward (EW) of the auroral oval. A subset of the MITs is associated with sub-auroral ion drift (driven by a poleward E-field) events (SAIDs) or sub-auroral polarization streams (SAPSs). A heat-induced upward drift of plasma is believed to contribute to the formation of the deepest SAPS troughs. MIT's position is known to depend on magnetic local time (MLT) and geomagnetic activity, e.g., [RD-3].

The MIT associated Te peak is believed to be the result of several factors. The main contributions are from the ring current (heat conduction, energy redistribution through soft precipitation and wave propagation along the field lines), decreased cooling (due to decreased density) [RD-5]. During SAID and SAPS events the frictional heating is considered as the dominant source of the extra heat.

Both the EW edge [RD-3][RD-6] of the MIT and the trough minimum [RD-8] or both [RD-9] were suggested as possible ionospheric signatures of the PP, while others found the relation of the MIT to the PP more complex [RD-10]. The poleward (PW) edge was found to be closely coincident with the EW edge of the auroral oval.

3.2 The low-latitude boundary of SSFACs and its relation to the PP

A new PP location proxy based on SSFAC signatures observed at LEO was introduced by [RD-1] who found a very close coincidence between the PP location and the EW boundary of sub-auroral SSFACs (as mapped onto the magnetic equatorial plane along IGRF field lines). This relation is the strongest in the post-midnight MLT sector [RD-1][RD-2]. Large-scale FACs are driven by the merging/convection E-field, dominantly in the polar region. The inner magnetosphere, the region where corotation dominates is shielded from the convection E-field. Consequently, convection E-field-driven FACs flow outside the shielded plasmasphere, i.e., PW of the PP footprint in the topside ionosphere. During disturbed times small-to-medium-scale electric fields (like the SAPS associated SAPS-E-field) also drive currents in the plasmasphere boundary layer. SSFACs could also be related to soft precipitation or some not-yet-identified Alfvén wave phenomena. Although many of the details of these processes need further investigation, CHAMP and Swarm observations clearly demonstrated that in the post-midnight sector, where the plasmasphere is trimmed by the increased convection and SAPS E-field during geomagnetic disturbances, the two boundaries, namely the PP, and the EW boundary of SSFACs lie close to each other. This was demonstrated not only on a statistical basis but also through one-to-one comparisons. As demonstrated by [RD-2] we can make use of this finding to derive a PP location proxy from the Swarm FAC density product.

Another outcome of the previous studies [RD-1][RD-2] was that for a given level of geomagnetic activity the SSFAC EW boundary - as mapped on the equatorial plane along field lines - could be well approximated by a

simple circle. The circular shape, i.e., a Kp-dependent but MLT independent radius means that the boundary reacts to changes in geomagnetic activity simultaneously at all MLTs. Although the shape of the SSFAC boundary is different from the shape of the PP (e.g., the PP typically has a bulge near dusk), the two boundaries were found to be dynamically coupled in the post-midnight sector. The circular shape of the SSFAC boundary also suggests that the boundary is related to the drift path of some particle population. The fact that the SSFAC boundary changes simultaneously at all MLTs, and that it coincides with the PP near midnight, makes Swarm suitable to monitor continuously the night side dynamic processes that form the PP. By the use of a boundary model, the midnight position of the SSFAC boundary can be derived from the observation of the same boundary at any MLT. The resulting value (after some adjustment based on calibration with validating PP positions) is what we call the midnight PP index.

As shown by [RD-2], the variation of the dayside true PP position correlates with the SSFAC index evolution observed a few hours earlier in the post-midnight sector. The lag time given by the cross-correlation equals the time passed since ~6 MLT. This is the result of corotation: the new PP shaped in the post-midnight sector is carried to the dayside by corotation. Hence the midnight PP index can be utilized in the future as a base for a new technique to reconstruct the shape (location as a function of MLT) of the main plasmasphere.

3.3 Previous attempts

In spite of the increasing number of papers dealing with the statistical analysis of MIT, there have been only a few attempts to develop fully automated algorithms for MIT detection. All approaches started from the quasi-definition of the MIT that describes it as depleted zone where the plasma density drops by a factor of X within a latitude range Y. Algorithms then look for the first (moving PW) location where this criterion is fulfilled or where the local density gradient exceeds a pre-defined threshold [RD-6] that corresponds to a similar density drop (i.e., X/Y). This approach is used to find the EW wall of the MIT. In this method, the subsequent local minimum is taken as the bottom of the trough (MIT minimum). We found that this approach often fails to detect the MIT, since the EW wall of the MIT is often not well-defined.

Others first took the minimum in a predefined magnetic latitude range (e.g., 45°-70°) as the trough minimum [RD-7], or a range minimum with an associated Te peak [RD-4], then defined the wall positions as the closest locations where the density equals the limited-range profile average [RD-7]. This approach may easily detect the MIT PW of the true MIT (especially in Ne), since the MIT do not necessarily coincide with the range minimum.

Every method has its advantages and weaknesses. Only a few of them are described as fully automated, due to the difficulties, most of them involved human control in some way. [RD-3] e.g., mentions that in an earlier study, they “also tried an automated procedure to identify latb [the location of the EW wall – BH] but were not satisfied with the results. It appears that the pattern recognition capability of the human brain is unsurpassed.”

The MIT algorithm used here is an improved version of the algorithm developed in the EPHEMERIS project (ESA contract No. 4000128162/19/I-DT). The improvements include the complete re-formulating of the algorithm based on a different detection strategy (that starts from gradients), involving complementary information from other Swarm products and an improved utilisation of the temporal evolution of the MIT throughout the detection process.

The SSFAC boundary detection introduced here is based on the algorithm developed and described by [RD-1] and [RD-2]. The main improvements come from the utilisation of other collocated, simultaneous Swarm observations that led to the increase in detection efficiency, to the increase of MLT coverage toward daytime.

The SSFAC boundary model that is fundamental for the derivation of the midnight PP index is being updated. The update will make also use of CHAMP data to reach a better coverage of highly disturbed periods.

4 Algorithms Description

The development of the new products is based primarily on historical data. However, we are targeting quasi real-time product provision for space weather now-casting and forecasting, hence the procedures have to be designed so that the whole processing chain can be executed within a few minutes once new data are available. For all the three products, the boundary detection begins with the analysis of latitudinal (in QD magnetic latitude sense) profiles of the variables considered. In each case, the detection starts at a fixed low magnetic latitude (30°) and we move PW until the boundary is found.

4.1 MIT detection based on the LP Ne and Te observations

In the following, the MIT detection process based on LP data is summarised (see also Figure 4-1 presenting the process in a flowchart).

4.1.1 Reading the data

Input data (EFIx_LP L1b product) for the day considered are read from the source cdf file. The daily data are complemented by the last/first segment fragment (from/to the last/first magnetic pole crossing) of the previous/consecutive day, respectively, so that the daily data contains complete pole-to-pole orbits. At the same time, the first orbit fragment is dropped, since it is analysed together with data of the previous day. The orbit counter is read from the AUXxORBCNT product files.

4.1.2 Main steps of the detection process

4.1.2.1 *Calculation of auxiliary data*

The calculation of quasi-dipole coordinates, the L-values ($L = 1/\cos^2 \varphi$, where φ is the QD-latitude), magnetic local time (MLT) and solar zenith angle (SZA) is done for all data points separately. The applied routines are the qdipole routine (written and maintained by N. Olsen, DTU) and the solar_zenith_angle routine (by P. Ritter, GFZ and N. Olsen, DTU).

4.1.2.2 *Segmentation of the data into quarter of orbits*

Based on the magnetic coordinates, all full Swarm orbits are divided into four segments that are numbered from 1 to 4 (denoted by QR, see section 4.1.2.7). The sequence of the four segments is as follows:

1. Ascending orbit, northern magnetic hemisphere (i.e., from magnetic equator to magnetic north pole);
2. Descending orbit, northern magnetic hemisphere (i.e., from magnetic north pole to magnetic equator);
3. Descending orbit, southern magnetic hemisphere (i.e., from magnetic equator to magnetic south pole);
4. Ascending orbit, southern magnetic hemisphere (i.e., from magnetic south pole to magnetic equator).

Here, the magnetic north/south pole is the position of the Swarm orbit with the largest QD latitude value.

4.1.2.3 *Interpolating missing and flagged values*

All of the input data need some pre-processing before they can be applied for the desired purposes. First, missing (gaps lasting for a few seconds) and flagged values (depending on the flag) are interpolated. For Ne and Te, only values with flags (Flags_Ne and Flags_Te) below 30 are used. This value is based on LP Measurement flag, Flags_XX, definition (Table 6-4 in [AD-4]):

10-19 Nominal data, error estimate applies;
20-29 Nominal data, but errors estimate do not apply/are not yet determined;

30-39 An error was detected, data may still be usable, see below;

>= 40 Unusable data, please discard.

4.1.2.4 *De-noising Te*

The Te data set of the Langmuir probe suffers from high noise level, especially at high latitudes, but occasionally also at mid and low latitudes. The noise features include unphysical spikes, base line jumps and broad band noise. First, the largest spikes are removed in an iterative process, gradually decreasing the spike threshold (10 000 K, 10 000 K, 5 000 K, 2 500 K and 1 000 K). Further outliers (spikes) are removed as follows. The data are smoothed by applying a 7-point (3.5 s) boxcar averaging. Then residuals and the median absolute deviations (MAD) are calculated. Data points with absolute residuals greater than 6*MAD are considered outliers and replaced by interpolated values.

4.1.2.5 *Filtering*

logNe=log10(Ne) and Te are low-pass filtered by applying a 3-order Butterworth filter with a corner frequency at 31.25 mHz (= 1/32 Hz). The resulting filtered data are denoted by logNe_f and Te_f, respectively.

4.1.2.6 *Calculating the first and second derivatives of logNe and Te*

The first and second derivatives of Te_f and logNe_f and TEC along the latitudinal profile are calculated as grad_x = δx/δmlat and gradgrad_x = grad_x/δmlat, respectively, where x stands either for Te_f or logNe_f. Then these values are low-pass filtered again using the same low-pass filter as in the previous step. Hereafter, grad_x is also referred to as the slope of the profile.

4.1.2.7 *Analysis of a single Ne profile*

The first pole-to-pole orbit segment is taken. The flight direction (*DIR*) is calculated. *NS* identifies the hemisphere, it takes the value of +1/-1 for the norther/southern hemisphere, respectively. $NS * DIR$ is then +1/-1 for PW/EW orbit segments. The orbit quarter identifier (QR, see section 4.1.2.2) is calculated as $QR = -NS - |NS + DIR|/2 + 3$, where | | stands for absolute value.

The logNe_f profile (restricted to the QD latitude range 30°-80°) is checked first for significant slopes, both PW positive and PW negative ones. The slopes along the profile are mostly PW negatives, since the density decreases from low toward high latitudes. The first significant increase is typically associated with the PW wall of the MIT, while a relatively steep decrease is expected at the EW wall of the MIT. A PW positive/negative slope is considered significant when its steepest point is steeper than $\log_{10}(1.11)$ and steeper than 50%/75% of the steepness of the steepest slope along the profile, respectively. If the first (i.e., at lowest latitude) significant slope is positive, the steepest negative slope EW of it is also added to the set of the selected “steep” slopes, even if its maximum steepness is below the threshold. This is because we are looking for density depletions, i.e., a minimum value between a negative and a positive slope and this step takes into account that the EW wall is not always well defined.

All the selected slopes are represented by their steepest points. Locations, where a PW negative slope is followed by a PW positive slope are the candidates for the MIT detection process. The slopes are the candidates of the walls of the MIT candidate. The walls may be a combination of more steeper slope sections separated by less steep sections. Moving PW, the EW wall starts at the first significant density decrease and lasts until the last significant decrease before the MIT minimum is reached, while the PW wall is the first significant density increase right after the MIT minimum.

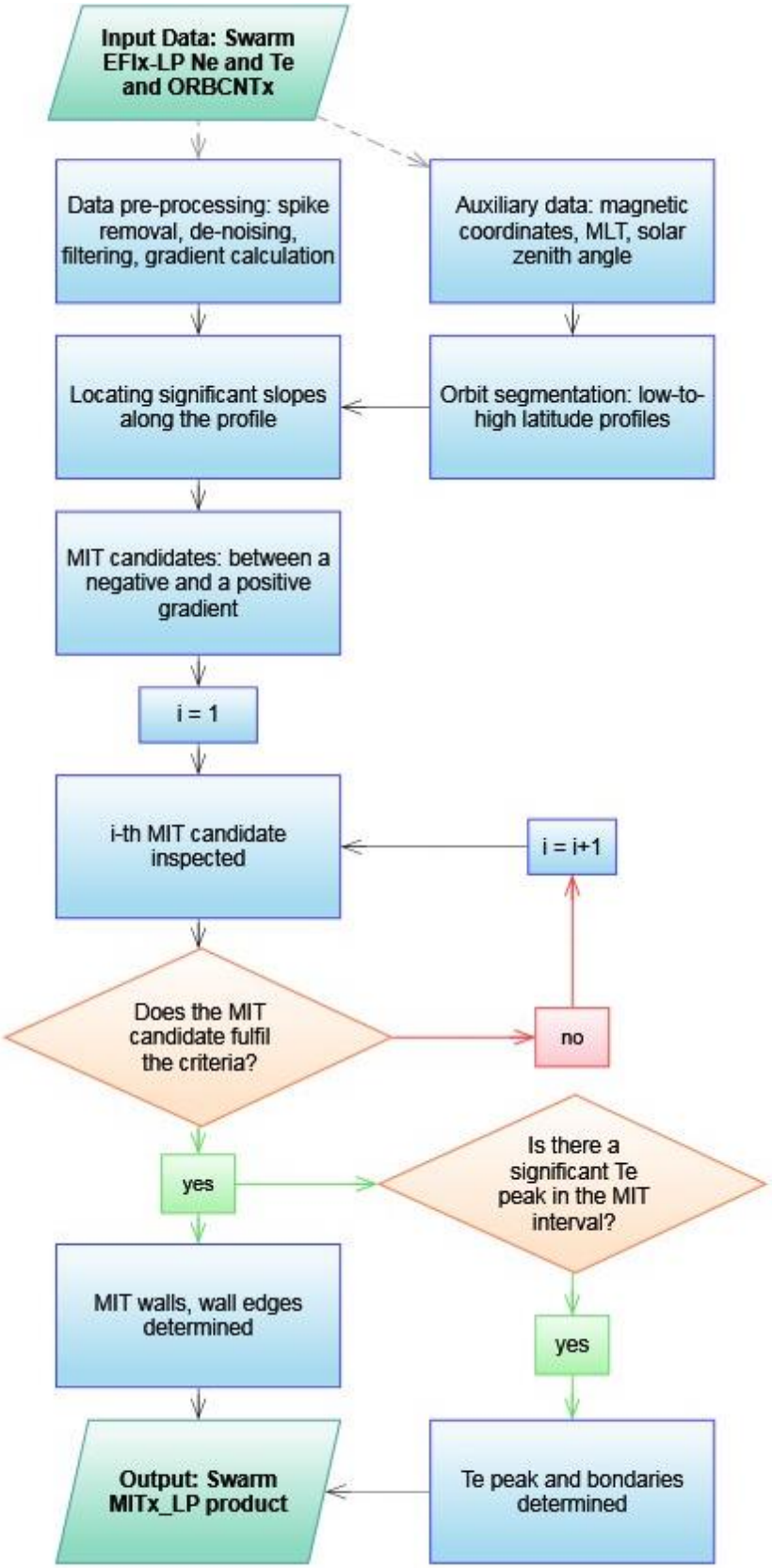

Figure 4-1 Flowchart showing the main steps of MIT detection in LP data.

If the EW edge of the EW wall is on a PW negative slope (typically this is the case) the algorithm makes attempt to extend the EW wall in the EW direction. It moves EW while the sign of the slope remains the same (negative), then checks the minimum of the second derivative in the extension interval. If this value is smaller than at the previously determined EW edge and the mean of the first gradient is greater than half of the gradient at the EW edge then this new location is selected as the new EW edge position. Under appropriate conditions all the other wall edges are extended in a similar way.

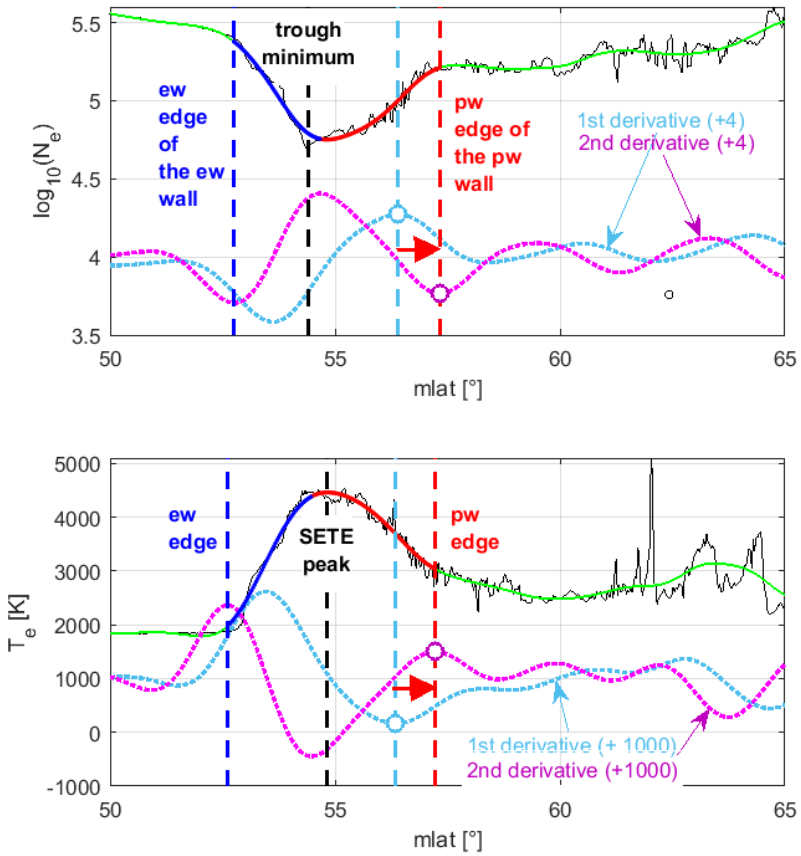

Figure 4-2 An example for the derivation of the MIT (upper panel) and SETE (lower) edges. See text for further explanation.

Finally, all the wall edges are defined by an extreme of the second derivative of the density profile. E.g., the EW/PW edge of the EW wall is defined by a minimum/maximum of the second derivative EW/PW of the steepest point (i.e., the minimum of the first derivative) (see the upper panel in Figure 4-2).

The minimum between the walls is the trough (MIT) minimum (depicted by a vertical black dashed line in Figure 4-2 upper panel). The boundaries (or walls) are found based on the first and second derivatives (light blue and magenta dotted curves) of logNe_f. The localisation of the walls starts from the above selected steepest points of the minimum bounding walls. E.g., to determine the PW edge of the PW wall we move PW (as shown by the red arrow in Figure 4-2 upper panel) of the steepest point of the PW wall (depicted by the vertical dashed light blue line at the maximum of the first derivative of logNe_f) until we reach a minimum (marked by a dashed red line) in the second derivative (green dotted curve). This is the point along the slope where the change of the steepness is the fastest. This point is taken as the PW edge of the PW wall. The EW edge of the same (PW) wall is found similarly, but now moving EW from the same starting point until a local maximum in the second derivative of logNe is reached (not shown). In case of a V-shape trough, this point

will be very close to or identical with the trough minimum. The EW wall is determined in the same way. The walls are deter-mined for each candidate, so that their properties, the selection criteria are based on could be calculated.

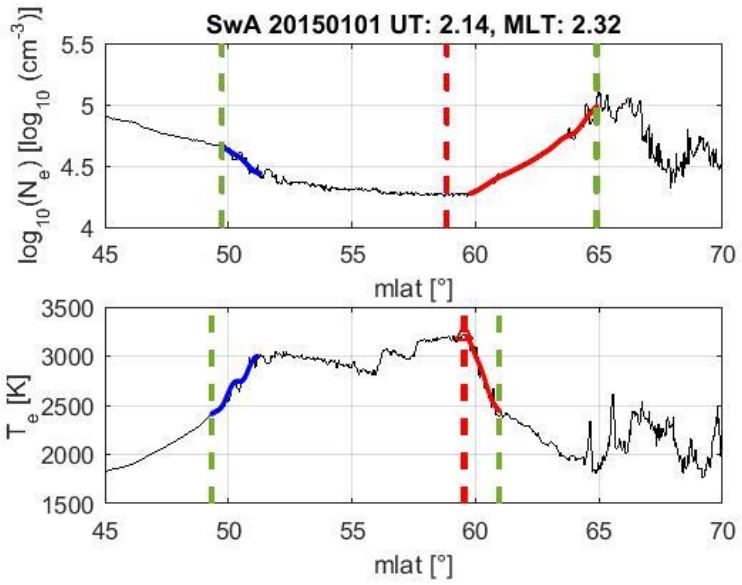

Figure 4-3 An example for a more complex MIT as wide density depletion (top) with the associated structure in Te (bottom). Green vertical dashed lines depict the MIT/SETE edges, while the red vertical dashed lines mark the MIT minimum and SETE peak.

SETE edges are found in a similar way (see Figure 4-2 lower panel) but for SETE only the outer edges are recorded.

The shape of the MIT can be more complex, an example is presented in Figure 4-3, where the EW and PW edges do not touch each other, they rather form a U-shape trough.

Only candidates with solar zenith angle > 90° are investigated further. The first (in latitude sense) one of these is tested. The selection criteria include the height of the EW and PW walls, the depth to width ratio, etc. It is also required that the trough minimum density is below the 40°-70° latitude-range-averaged density. The PW edge of the MIT should be EW of the EW edge of the auroral oval (from AOB product).

4.1.2.8 *Check for a nearby Te peak*

The MIT is known to be associated with a zone of increased electron temperature termed SETE (sub-auroral electron temperature enhancement) by [RD-5]. First the Te maximum within the investigated MIT candidate interval is taken (see Figure 4-3, example for a more complex MIT as wide density depletion (top) with the associated structure in Te (bottom)). The Te peak is determined in a somewhat (by 0.5 degrees on both sides) extended MIT interval. Maxima found at the edges of the extended MIT interval are excluded from further investigation, and the largest inner local maxima is considered instead. If more equal peaks are found the one at the lowest latitude is kept. The Te peak is considered significant if it is above the 40°-70°latitude range average. The edges of the enhancement are determined in a similar way as for the density depletion. However, the applied steepness threshold is much lower (20 %) than for the density profiles reflecting the often-gradual Te increase within the SETE. Slopes steeper than the threshold represent the candidates for the SETE boundaries.

4.1.2.9 *Evaluation of the MIT candidates*

After the first MIT and the associated SETE is available for analysis, the candidate is evaluated. A candidate is accepted as a likely MIT (SETE) if

1. the detection is made at SZA greater than 90° (i.e., on the night side[1] or when the S/C is lit from below),
2. the trough minimum is below the 40°-70° range mean of the density, and
3. at least one of the following three criteria is fulfilled:
4. the MIT has a high PW wall (i.e., trough minimum < 0.5625*density at the PW edge of the PW wall), or
5. the MIT has a high EW wall (i.e., trough minimum < 0.5625*density at the EW edge of the EW wall), or
6. the MIT has a less high wall (i.e., trough minimum < 0.75*density at the PW edge of the PW wall) but fulfils the shape condition (trough minimum < $10^{-PWW/20}$*density at the PW edge of the PW wall, where PWW is the width of the PW wall in degrees).

If as a result of the evaluation, the MIT candidate is accepted, all the MIT properties are saved and the process continues with the following equator-to-pole density profile. Otherwise, if the acceptance criteria are not fulfilled, the detection process restarts but now starting from the PW edge of the rejected MIT candidate.

4.1.3 The MIT product output properties

The derivation of the MIT properties (as defined in [AD-2]) is as follows:

Variable Name	Type	Dim	Unit	Description	Comment
Timestamp	CDF_EPOCH	1		Time of observation, UTC	The time of the MIT minimum observation
Counter	CDF_UINT4	2	N/A	Swarm orbit counter and quarter orbit (four per Swarm orbit) counter	The orbit counter from the ORBCNT product (section 4.1.1), and the orbit quarter identifier QR as described in section 4.1.2
Latitude	CDF_DOUBLE	1	deg	Position of the MIT minimum in ITRF – Geocentric latitude	
Longitude	CDF_DOUBLE	1	deg	Position of the MIT minimum in ITRF – Geocentric longitude	
Radius	CDF_DOUBLE	1	m	Position of the MIT minimum in ITRF – Geocentric radius (from the Earth centre)	
Latitude_QD	CDF_DOUBLE	1	deg	QD latitude of the MIT minimum	
Longitude_ QD	CDF_DOUBLE	1	deg	QD longitude of the MIT minimum	
MLT	CDF_DOUBLE	1	h	Magnetic Local Times of the MIT minimum	
L_value	CDF_DOUBLE	1	N/A	L-value of the MIT minimum	
Ne	CDF_DOUBLE	1	cm^{-3}	LP electron densities of the MIT minimum	Filtered electron densities

[1] The sunrise/sunset angle at the altitude of the satellite is greater than on the ground. At 500 km altitude the threshold SZA is 112° $(180° - \sin^{-1}(R/(R+h)))$.

Variable Name	Type	Dim	Unit	Description	Comment
Te	CDF_DOUBLE	1	K	LP electron temperatures of the MIT minimum	Filtered electron temperatures
SZA	CDF_DOUBLE	1	deg	Solar zenith angles of the MIT minimum	
Depth	CDF_DOUBLE	1	cm^{-3}	Depth of the MIT	The difference of the mean of the Ne values at the MIT edges and at the MIT minimum $(Ne_1 + Ne_4)/2 - Ne_{MIT}$
DR	CDF_DOUBLE	1	%	Relative change in density within the MIT	Density drop rate, i.e.: $2Ne_{MIT}/(Ne_1 + Ne_4)$
Width	CDF_DOUBLE	1	deg	Width of the MIT calculated from QD latitudes	Width of the MIT calculated from QD latitudes: $Latitude\_QD_4 - Latitude\_QD_1$
dL	CDF_DOUBLE	1	N/A	Width of the MIT calculated from L-values	width of the MIT calculated from L-value: $L_4 - L_1$
PW_Gradient	CDF_DOUBLE	1	log(cm^{-3})/deg	Change in log electron density at the poleward wall of the MIT divided by QD latitude difference	This is a positive gradient $\frac{\log_{10} Ne_4 - \log_{10} Ne_3}{Latitude\_QD_4 - Latitude\_QD_3}$
EW_Gradient	CDF_DOUBLE	1	log(cm^{-3})/deg	Change in log electron density at the equatorward wall of the MIT divided by QD latitude difference	This is a negative gradient $\frac{\log_{10} Ne_2 - \log_{10} Ne_1}{Latitude\_QD_2 - Latitude\_QD_1}$
Quality	CDF_UINT4	8	N/A	Characterizes the detection quality of the MIT as a whole	See section 4.3
Timestamp_ID	CDF_EPOCH	7		Vector of times of observation, UTC	
Latitude_ID	CDF_DOUBLE	7	deg	Vector of positions in ITRF – Geocentric latitude	
Longitude_ID	CDF_DOUBLE	7	deg	Vector of positions in ITRF – Geocentric longitude	
Radius_ID	CDF_DOUBLE	7	m	Vector of positions in ITRF – Geocentric radius (from the Earth centre)	
Latitude_QD_ID	CDF_DOUBLE	7	deg	Vector of QD latitudes	
Longitude_QD_ID	CDF_DOUBLE	7	deg	Vector of QD longitudes	
MLT_ID	CDF_DOUBLE	7	h	Vector of Magnetic Local Times	
L_value_ID	CDF_DOUBLE	7	N/A	Vector of L-values in Earth radii	
Ne_ID	CDF_DOUBLE	7	cm^{-3}	Vector of LP electron densities	Filtered electron densities
Te_ID	CDF_DOUBLE	7	K	Vector of LP electron temperatures	Filtered electron temperatures
SZA_ID	CDF_DOUBLE	7	deg	Vector of solar zenith angles	
Position_Quality_ID	CDF_UINT4	7	N/A	Vector of quality indicators (TBD) characterizing the detection quality of each single positions	See section 4.3.1

In the above list the meaning of ID is:

1 - LP MIT EW edge of the EW wall ‘ee’;
2 - LP MIT PW edge of the EW wall ‘ep’;
3 - LP MIT EW edge of PW wall ‘pe’;
4 – LP MIT PW edge of the PW boundary ‘pp’;
5 - LP Te EW bounding position ‘te’;
6 - LP Te peak position ‘tk’;
7 - LP Te PW bounding position ‘tp’.

E.g., Longitude_QD_4 is the QD longitude of the MIT PW edge observation, Ne_3 is the LP density at the EW edge of the PW MIT wall, Te_6 is the peak temperature, etc.

4.2 Definition of the MITx_LP quality flags

The Quality parameter is a vector of eight flag values defined below in the order of their position in the Quality vector. The first of these is the main flag. For scientific case/statistical studies the use of data with main flag > 2/1 is recommended.

Some of the quality flags are based on a comparison between different boundaries (their L-difference) or temporal changes of their position (L-value). The smaller the difference or change, the higher the flag value is. More precisely, the flag values are based on the statistics of these differences. The difference/change is flagged according to which of the intervals defined by the [0 0.025 0.10 0.25 0.75 0.90 0.975 1] quantiles of the differences it fits in. The flag values associated with the [(0-0.025), (0.025-0.10), (0.10-0.25), (0.25-0.75), (0.75-0.90), (0.90-0.975), (0.975-1)] quantile intervals are -1, 1, 2, 3, 2, 1, -1, respectively. Thus 50% of the detections will have the flag value 3, further 30%/15%/5% will obtain flag values 2, 1, and -1, respectively. The flag is set to 0 when the information needed to define the flag is missing. In some cases, the difference, the flagging is based on strongly depends on MLT. In these cases, first, this MLT-dependence is removed from the data, and then this cleaned difference (the residual) is used to define the flag.

In the following, for each flag that is based on the quantile-based qualifications, the applied quantile values are given in the vector QQ. Whenever a de-trended difference is used for flag definition, the linear trend removed is also given. The quantile intervals were derived from an analysis similar to that introduced in section 4.4 of the Validation Report but on an earlier and more complete (2014-2019) version of the product.

Flag_MIT

is the main flag characterising the overall quality of the product. Hence it is derived from the other flags and other information, its derivation is described at the end of this chapter. The possible values of the flag and their meaning are 3: highest quality, 2: fair quality, 1: uncertain detection, 0: no quality information available, -1 – likely false positive detection.

Flag_PPI

is based on the L-value distance between the SSFAC boundary and the MIT minimum. Since this difference has a strong MLT-dependence, first this trend is removed. Then the de-trended difference is used to define Flag_PPI as described above.

trend: $dL_{MITxLP-PPIxFAC} = -0.178 \cdot MLT^* + 0.14$ Eq. 4.2-1

quantiles: QQ_PPI = [-inf, -0.95, -0.53, -0.22, 0.34, 0.64, 1.06, inf]

Flag_ROC

is based on the rate of change (ROC, i.e., change per orbit) of the L-value of the MIT minimum. The flag values are derived from the ROC values as described above. First the closest (in time) of the three preceding observation is used to define the ROC and then this flag (Flag_ROCa). Then in a similar way, a flag value corresponding to the change be-tween the current and the following orbit (Flag_ROCp) is calculated. The maximum of the two flag values (Flag_ROCa and Flag_ROCp) defines the value of Flag_ROC. Whenever this flag has a high value (3 or 2), it means that the consecutive observations support each other. In a dynamic situation, at sudden changes, this flag can be low. Hence this flag alone cannot be used to assess the overall quality of the MIT detection.

quantiles: QQ_ROC = [-inf, -1.00, -0.59, -0.25, 0.25, 0.50, 0.84, inf]

Flag_TEC

is based on the L-value distance between the MIT minima derived from LP and TEC observations. This difference slightly depends on L, thus first this trend is removed. Then the de-trended difference is used to define Flag_TEC as described above.

trend: $dL_{MITxLP-MITxTEC} = 0.007 \cdot MLT^* - 0.04$ Eq. 4.2-2

quantiles: QQ_TEC = [-inf, -0.60, -0.35, -0.18, 0.13, 0.37,0.77, inf]

Flag_Te

gives information on the relative position (L-value) of the Te peak wrt. the MIT. This flag is 3, when the Te peak is within the MIT and closer than 0.5 to the MIT minimum, otherwise if the peak is inside the MIT but the distance is greater than 0.5, the flag value is 2. A value 1 means the Te peak is outside the MIT but closer to its edge than 0.5. -1 indicates that the Te peak is further than 0.5 from the MIT.

Flag_AOB

depends on the mutual position of the AOB boundary and the MIT minimum (1: AOB is poleward of the MIT minimum, -1: otherwise).

Flag_WSA

is calculated from the solar zenith angle at the MIT minimum (3: SZA>110°; 2: 110≥SZA>100°, 1: 100≥SZA>90°; -1: SZA≤90°). The greatest value corresponds roughly to the SZA at sunset/sunrise at Swarm's altitude that is 110°/112° at 400/500 km altitude. The smallest value corresponds to the situation when the sunrays are parallel with the ionospheric layers.

4.2.1 Flag_MIT

Now we return to the definition of the main quality flag that assesses the overall quality of the product record. Whenever Flag_WSA = -1, Flag_MIT = -1, i.e., in the Weddell-See Anomaly region, the flag equals the Flag_WSA:

Flag_MIT = Flag_WSA (= -1).

If Flag_PPI=-1 OR L_MIT is EW of L_AOB-2 OR L_MIT>10 OR 10<MLT<14, then the detection is considered very low quality and removed from the product (close-to-noon observations at extremely high-L or well EW

of AOB or far from the SSFAC boundary). Here, and in the following, L_MIT and L_AOB stand for L_Value of MITx_LP, and L_Value of AOBxFAC, respectively.

When no information of SSFAC boundary is available (Flag_PPI=0), the dayside observations cannot be verified. The risk increases with decreasing SZA and approaching MLT noon.

If Flag_PPI=0 AND (L_MIT<3 OR L_MIT>6 OR 6<MLT<18) AND SZA<100°, then the detection is consid-ered very low quality and removed from the product (dayside observations at rather high or low L).

If Flag_PPI=0 AND (L_MIT<3 OR L_MIT>6 OR 6<MLT<18) AND SZA>=100°, then the detection is considered uncertain, hence

Flag_MIT = -1.

If Flag_PPI=0 AND 3<=L_MIT<=6 AND (MLT<=6 OR 18<=MLT), then Flag_MIT is estimated from Flag_ROC:

Flag_MIT = Flag_ROC-1.

When Flag_PPI>0 (MIT and the SSFAC boundary are at moderate distance) and Flag_ROC is defined (i.e., in most of the MIT detections), then these Flag_MIT mostly depends on these two flags.

If Flag_PPI>0 AND Flag_ROC>=0, then

Flag_MIT = max(Flag_PPI, Flag_ROC).

If Flag_PPI>0 AND Flag_ROC=-1, then

Flag_MIT = Flag_PPI – 1.

When Flag_PPI>0 (MIT and the SSFAC boundary are at moderate distance) and Flag_ROC is defined (i.e., in most of the MIT detections), then these Flag_MIT mostly depends on these two flags.

If Flag_PPI>0 AND Flag_ROC>=0, then

Flag_MIT = max(Flag_PPI, Flag_ROC).

If Flag_PPI>0 AND Flag_ROC=-1, then

Flag_MIT = Flag_PPI – 1.

In the following, based on further considerations, Flag_MIT is further refined. Flag_Te and Flag_TEC are used to strengthen (increase) an already positive main flag if the SETE and TEC-based MIT observations confirm the LP-based MIT detection (i.e., they lie close to each other).

If Flag_MIT>0 AND max(Flag_Te,Flag_TEC)>Flag_MIT, then

Flag_MIT = Flag_MIT + 1.

The less certain detections (Flag_MIT<3) are further checked. These observations may be qualified questionable if they were made at very low or very high L. In other words, for the extreme cases, only the highest quality detections have positive main flag.

If {1<=Flag_MIT<=2 AND (L_MIT<2 OR 8<L_MIT<=10)} OR {0<=Flag_MIT<=1 AND (2<=L_MIT<3 OR 6<L_MIT<=8)}, then

Flag_MIT = -1.

If 0<=Flag_MIT<=1 AND (L_MIT<2 OR 8<L_MIT<=10), then the detection is considered poor quality and removed from the product.

4.2.2 Position_Quality_IDs

Position_Quality_ID is a vector of seven elements corresponding to the seven boundary positions de-fined for each MIT observations. The seven positions are: 1 – LP MIT EW edge of the EW wall 'ee'; 2 – LP MIT PW edge of the EW wall 'ep'; 3 – LP MIT EW edge of PW wall 'pe'; 4 – LP MIT PW edge of the PW wall 'pp'; 5 – LP Te equatorward bounding position 'te'; 6 – LP Te peak position 'tk'; 7 – LP Te poleward bounding position 'tp'. The corresponding quality flags are depicted as follows:

Position_Quality_ID = [Flag_MIT_ee, Flag_MIT_ep, Flag_MIT_pe, Flag_MIT_pp, Flag_SETE_e,

Flag_SETE, Flag_SETE_p],

where

Flag_MIT_ee [*Position_Quality_1*]

First, *Q* is calculated as

Q = 100*gradgrad_logNe_f_ee*mean(NS*grad_logNe_f)_ew/mean(logNe_f)_ew,

where xxx_ee is the value of xxx at the EW edge of the EW wall, mean()_ew stands for the interval mean taken within the EW wall. *Q*s less than 1/8 are all set to 1/16, *Q*s > 1 are all set to 1. Then Flag_MIT_ee is calculated as

Flag_MIT_ee = 3 + fix(log2(*Q*));

This gives a value between 1 and 3 for *Q* > 1/8, and -1 otherwise. A larger value corresponds to a steeper wall and a sharper contrast in steepness at the outer edge of the wall.

Flag_MIT_ep [*Position_Quality_2*]

First, *Q* is calculated as

Q = mean(NS*grad_logNe_f)_ew/ min(NS*grad_logNe_f)_ew,

where min()_ew stands for the interval minimum taken within the EW wall. *Q*s are treated the same way as above to derive the quality flag

Flag_MIT_ep = 3 + fix(log2(*Q*));

This gives a value between 1 and 3 for *Q* > 1/8, and -1 otherwise. A larger value corresponds to less structured (more linear) wall.

Flag_MIT_pe [*Position_Quality_3*]

If L_value_3 > 10.5 then Flag_MIT_pe = -1.

Otherwise, first, *Q* is calculated as

Q = mean(NS*grad_logNe_f)_pw/ max(NS*grad_logNe_f)_pw,

where max()_pw stands for the interval maximum taken within the PW wall. *Q*s are treated the same way as above to derive the quality flag

Flag_MIT_pe = 3 + fix(log2(*Q*));

This gives a value between 1 and 3 for *Q* > 1/8, and -1 otherwise. A larger value corresponds to less structured (more linear) wall.

Flag_MIT_pp [*Position_Quality_4*]

If L_value_4 > 12.5 then Flag_MIT_pp = -1.

Otherwise, first, *Q* is calculated as

Q = -100*gradgrad_logNe_f_pp*mean(NS*grad_logNe_f)_pw/mean(logNe_f)_pw,

where xxx_pp is the value of xxx at the PW edge of the PW wall, mean()_pw stands for the interval mean taken within the PW wall. *Q*s are treated the same way as above to derive the quality flag

Flag_MIT_pp = 3 + fix(log2(*Q*));

This gives a value between 1 and 3 for *Q* > 1/8, and -1 otherwise. A larger value corresponds to a steeper wall and a sharper contrast in steepness at the outer edge of the wall.

Flag_SETE_e [*Position_Quality_5*]

First, *Q* is calculated as

Q = mean(NS*grad_Te_f)_ew/max(NS*grad_Te_f)_ew,

*Q*s are treated the same way as above to derive the quality flag

Flag_SETE_e = 3 + fix(log2(*Q*));

This gives a value between 1 and 3 for *Q* > 1/8, and -1 otherwise. A larger value corresponds to less structured (more linear) wall.

Flag_SETE [*Position_Quality_6*]

is defined the same way as Flag_MIT, only the location of the L-value of the Te peak has to be substituted to replace the L-value of the MIT minimum. Flag_SETE is the 6th flag of Position_Quality_ID.

Flag_SETE_p [*Position_Quality_7*]

If L_value_7 > 12 then Flag_SETE_p = -1.

Otherwise, first, *Q* is calculated as

Q = mean(NS*grad_Te_f)_pw/min(NS*grad_Te_f)_pw,

*Q*s are treated the same way as above to derive the quality flag

Flag_SETE_p = 3 + fix(log2(*Q*));

This gives a value between 1 and 3 for *Q* > 1/8, and -1 otherwise. A larger value corresponds to less structured (more linear) wall.

4.3 MIT detection based on the GPS TEC observations

The detection of the MIT in TEC data follows a similar logic as in Ne profiles. There are some important differences, however. First, unlike in-situ LP electron densities, TEC data are spatially integrated values. The TEC value depends not only the time and location of the observation, but also on the direction of the line of sight between Swarm and the GPS satellite. TEC values derived from low elevation measurements have generally larger errors. When Swarm crosses a density structure such as the MIT, the shape and location of the observed structure also depends on the relative location of the two satellites. Swarm sees several of the 32 GPS satellites at any time instant, all in different directions. Hence the MIT may appear at different latitudes with different depth in TEC profiles inferred from signals of different GPS satellites. The deepest trough observation is expected along the lines of sight aligned with the density structure, i.e., with the geomagnetic field line. Having several simultaneous observations increase the probability of a successful

detection. On the other hand, simultaneous observations can also be used to cross-check the observation results.

On transforming the slant TEC data to vertical TEC values, several assumptions are made that are violated around the MIT. That is why we decided to use the absolute slant TEC data. Since for the detection the relative changes are more important than the absolute values, slant TEC data seem overall to be more appropriate. The elevation related inaccuracies are also less critical for the same reason. This has impact however, on the absolute TEC values included in the product.

However, since both the constellation of the GPS satellites and the position of the LEO satellite change in time, many of the GPS satellites can only be seen during a fraction of a pole-to-pole Swarm orbit. We can only use TEC time series that cover a wide latitude range (from low to high latitudes) for safe detection. This requirement also implies that near the edges of the orbit sections investigated, the GPS elevation will be below the optimum. This leads to further inaccuracies in the absolute values. On the other hand, GPS satellites that can be seen from all along the 50° latitude range are typically those with higher elevation (at least at some section of the profile).

4.3.1 Reading the data

TECxTMS L2 product input data for the day considered are read from the source cdf file. The daily data are complemented by the first segment fragment of the consecutive day, so that the daily data contains complete pole-to-pole orbits. At the same time, the first orbit fragment is dropped, since it is analysed together with data of the previous day. The orbit counter is read from the AUXxORBCNT product files.

4.3.2 Main steps of the detection process

The main steps of the process are presented in Figure 4-4, and described below.

4.3.2.1 *Calculation of auxiliary data*

For information on the calculation of magnetic coordinates, MLT, the L-value and solar zenith angles, see section 4.1.2.1.

4.3.2.2 *Segmentation of the data into quarter of orbits*

The same as described in section 4.1.2.2.

4.3.2.3 *Interpolating missing and flagged values*

No interpolation is applied for missing TEC values.

4.3.2.4 *De-noising*

No special de-noising is applied.

4.3.2.5 *Filtering TEC*

Due the integral nature of the TEC data, they are typically much smoother than the Ne time series therefore, no filtering is needed. Only the gradient time series (see below) are filtered (in the same way as Ne is filtered).

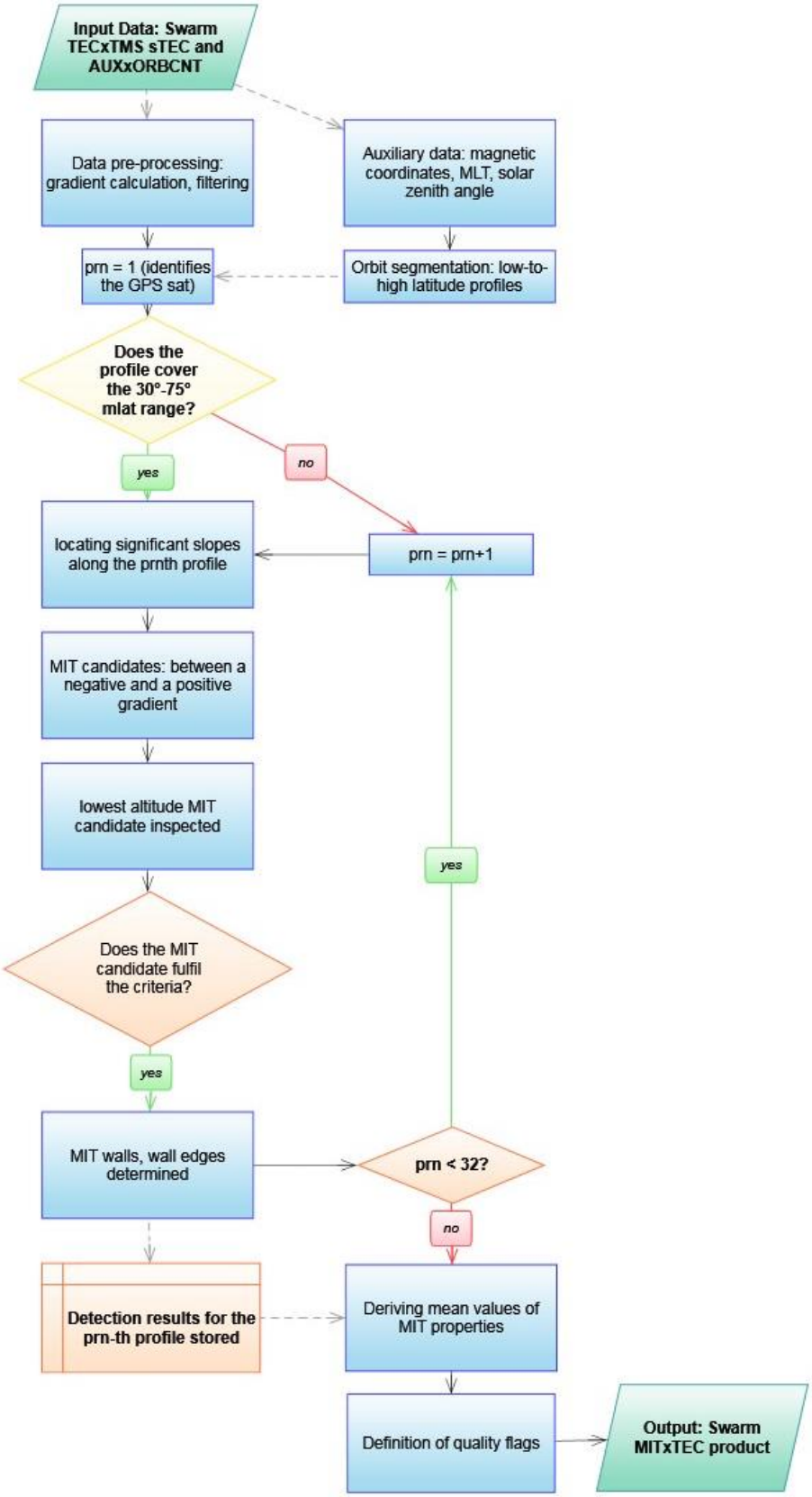

Figure 4-4 The main steps of the MIT detection in the TEC time series.

4.3.2.6 *Calculating the first and second derivatives of TEC*

The first derivatives of sTEC along the latitudinal profile are calculated as grad_TEC = δTEC/δmlat and gradgrad_TEC = grad_TEC/ δmlat, respectively. Then these values are low-pass filtered again.

4.3.2.7 *Analysis of a single TEC profile*

Equator-to-pole profiles of TEC data are analysed. TEC data belonging to different GPS satellites are analysed one-by-one. Only profiles covering the whole 30°-75° mlat range are analysed.

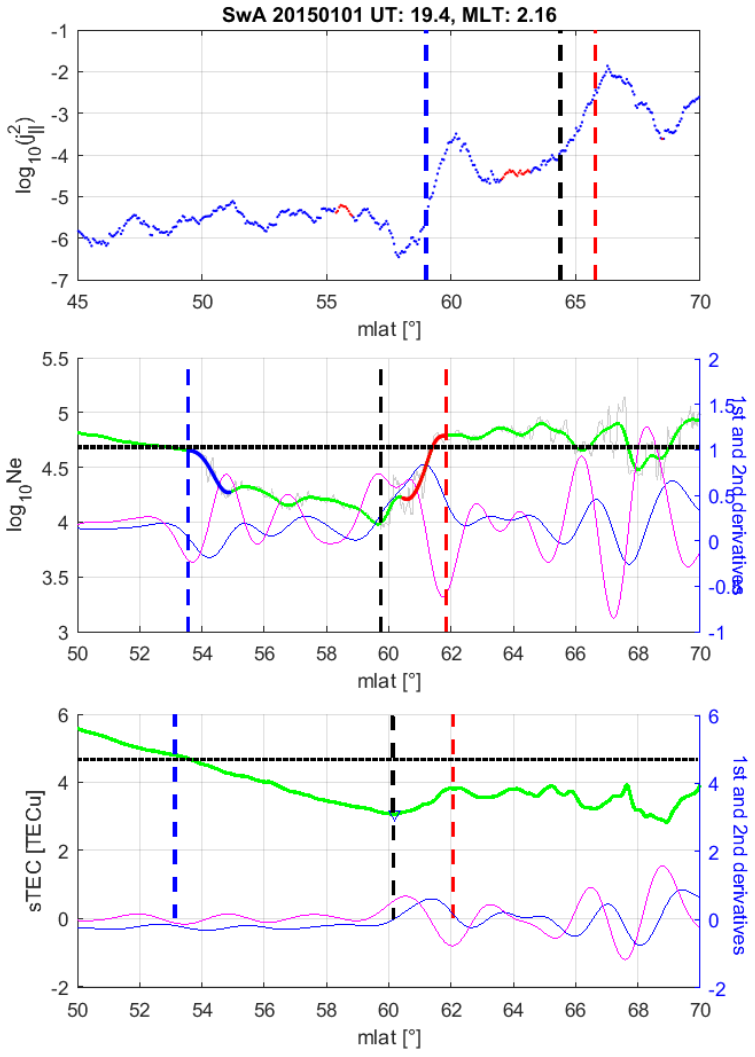

Figure 4-5 An example of the MIT detection in TEC depicted by a green line (bottom), with the simultaneous observation of the MIT in LP Ne shown as a green line (middle) and the SSFAC boundary (top). The blue and magenta curves in the middle and bottom plots are the first and second derivatives of logNe and TEC, respectively. The blue and red dashed lines in the same panels depict the equatorward and poleward edge of the MIT, respectively, while the vertical dashed lines in the same mark the detected MIT minimum. Thick black horizontal dotted lines represent the range (40°-70°) average of the corresponding parameter.

The procedure (the flowchart illustrating the main steps is shown in Figure 4-4) is very similar to the LP MIT detection. The profile (restricted to the magnetic latitude range [30°; φ_max], where $\varphi_{max} = \min(75°, \max(profile\ latitudes))$ is checked for significant positive and negative slopes in TEC. A slope is

considered significant when its maximum steepness is steeper than half of the steepness of steepest point along the investigated magnetic latitude range. The threshold is computed separately for positive and negative slopes. In any case, the minimum possible threshold is set to 0.25 TECU/deg. If the first (i.e., the lowest latitude) significant slope is found positive, the steepest negative slope EW of it is also selected, even if its maximum slope is below the threshold. This is again because we are looking for density depletions, i.e., a minimum value between a negative and a positive slope, and also because the EW wall is often poorly defined. All the detected significant slopes are represented by their steepest points. Intervals, where a negative slope is followed by a positive slope are the candidates for the MIT detection process. The slopes are the walls of the MIT candidate.

The minimum between the walls is the trough minimum (depicted by a black vertical dashed line in Figure 4-5, bottom panel). The boundaries (or walls) are found based on the first and second derivatives of TEC (blue and magenta curves). Similarly, to the detection in LP Ne, the process starts at the steepest points of the slopes. E.g., to determine the PW edge of the PW wall we move PW of the steepest point (i.e., the local maximum of the blue curve, the first derivative of TEC) until we reach a minimum (depicted by the vertical red dashed line) in the second derivative of TEC (the magenta curve). This is the point along the slope where the change of the steepness is the fastest. This point is taken as the PW edge of the PW wall. The EW edge of the same wall is found similarly, but now moving EW from the same point. In case of a V-shape trough, this point will be very close to or identical with the trough mini-mum. The EW wall is determined in a similar way. The walls are determined for each candidate, so that their properties the selection criteria are based on could be calculated.

Only candidates with solar zenith angle > 90° candidates are investigated further. The first (in latitude sense) one of these is tested. The selection criteria include the height of the EW and PW walls, the depth to width ratio. The trough minimum density is expected to be below the 40°-70° range average, the trough minimum cannot be PW of the profile (absolute) minimum. The PW edge of the MIT is expected to be EW of the EW edge of the auroral oval (from AOB product).

4.3.3 Comparing the MIT detections derived from the simultaneous TEC observations

Once all available GPS TEC time series are analysed, they are compared. Their mean (e.g., that of the minimum positions) is calculated and used as the product value. The scatter of the observations is used to derive a quality flag.

4.3.4 The MITxTEC product output properties

The derivation of the MITxTEC properties (as defined in [AD-2]) is similar to that of the MITx_LP product properties with the difference that all values below are the means of observations derived from parallel GPS TEC time series:

Variable Name	Type	Dim	Unit	Description	Comment
Timestamp	CDF_EPOCH	1		Time of observation, UTC	The time of the MIT minimum observation
Counter	CDF_UINT4	2	N/A	Swarm orbit counter and quarter orbit (four per Swarm orbit) counter	The orbit counter from the ORBCNT product (section 4.1.1), and the orbit quarter identifier QR as described in section 4.1.2
Latitude	CDF_DOUBLE	1	deg	Position of the MIT minimum in ITRF – Geocentric latitude	

Variable Name	Type	Dim	Unit	Description	Comment
Longitude	CDF_DOUBLE	1	deg	Position of the MIT minimum in ITRF – Geocentric longitude	
Radius	CDF_DOUBLE	1	m	Position of the MIT minimum in ITRF – Geocentric radius (from the Earth centre)	
Latitude_QD	CDF_DOUBLE	1	deg	QD latitude of the MIT minimum	
Longitude_QD	CDF_DOUBLE	1	deg	QD longitude of the MIT minimum	
MLT	CDF_DOUBLE	1	h	Magnetic Local Times of the MIT minimum	
L_value	CDF_DOUBLE	1	N/A	L-value of the MIT minimum	
TEC	CDF_DOUBLE	1	TECU	Total electron content of the MIT minimum	
SZA	CDF_DOUBLE	1	deg	Solar zenith angles of the MIT minimum	
Depth	CDF_DOUBLE	1	TECU	Depth of the MIT	The difference of the mean of the Ne values at the MIT edges and at the MIT minimum $(TEC_1 + TEC_4)/2 - TEC_{MIT}$
DR	CDF_DOUBLE	1	%	Relative change in density within the MIT	TEC drop rate*, i.e.: $2(TEC_{MIT} + 2)/(TEC_1 + TEC_2 + 4)$
Width	CDF_DOUBLE	1	deg	Width of the MIT calculated from QD latitudes	Width of the MIT calculated from QD latitudes: $Latitude\_QD_4 - Latitude\_QD_1$
dL	CDF_DOUBLE	1	N/A	Width of the MIT calculated from L-values	Width of the MIT calculated from L-values: L_4-L_1
PW_Gradient	CDF_DOUBLE	1	TECU/deg	Change in TEC at the poleward wall of the MIT divided by QD latitude difference	This is a positive gradient $\frac{TEC_4 - TEC_3}{Latitude\_QD_4 - Latitude\_QD_3}$
EW_Gradient	CDF_DOUBLE	1	TECU/deg	Change in TEC at the equatorward wall of the MIT divided by QD latitude difference	This is a negative gradient $\frac{TEC_1 - TEC_2}{Latitude\_QD_2 - Latitude\_QD_1}$
Quality	CDF_UINT4	8	N/A	Characterizes the detection quality of the MIT as a whole	See section 4.4
Timestamp_ID	CDF_EPOCH	4		Vector of times of observation, UTC	
Latitude_ID	CDF_DOUBLE	4	deg	Vector of positions in ITRF – Geocentric latitude	
Longitude_ID	CDF_DOUBLE	4	deg	Vector of positions in ITRF – Geocentric longitude	
Radius_ID	CDF_DOUBLE	4	m	Vector of positions in ITRF – Geocentric radius (from the Earth centre)	
Latitude_QD_ID	CDF_DOUBLE	4	deg	Vector of QD latitudes	
Longitude_QD_ID	CDF_DOUBLE	4	deg	Vector of QD longitudes	

* An offset (2 TECU) was applied when calculating DR to avoid division by close to zero values and/or negative DRs. Since the uncertainty of TEC is 2 TECU, TEC values below zero may occur near the MIT minimum. In such a case, the mean of the edges may be close to zero resulting in large DR values, both positive and negative. For the same reason, MIT minima at TEC<-1 TECU are flagged (flag_MIT = -1, see below).

Variable Name	Type	Dim	Unit	Description	Comment
MLT_ID	CDF_DOUBLE	4	h	Vector of Magnetic Local Times	
L_value_ID	CDF_DOUBLE	4	N/A	Vector of L-values in Earth radii	
TEC_ID	CDF_DOUBLE	4	TECU	Vector of TEC values	
SZA_ID	CDF_DOUBLE	4	deg	Vector of solar zenith angles	
Position_Quality_ID	CDF_UINT4	4	N/A	Vector of quality indicators characterizing the detection quality of each single positions	See section 4.4.2

In the above list the meaning of ID is:

1 - TEC MIT EW edge of the EW wall ‘ee’;
2 - TEC MIT PW edge of the EW wall ‘ep’;
3 - TEC MIT EW edge of PW wall ‘pe’;
4 – TEC MIT PW edge of the PW boundary ‘pp’.

E.g., Longitude_QD_4 is the QD longitude of the MIT PW edge observation, TEC_3 is the TEC at the EW edge of the PW MIT wall.

4.4 Definition of the MITxTEC quality flags

The Quality parameter is a vector of eight flag values defined below in the order of their position in the Quality vector. The first of these is the main flag. For scientific case/statistical studies the use of data with main flag > 2/1 is recommended.

Flag_MIT

is the main flag characterising the overall quality of the product. Hence it is derived from the other flags and other information, its derivation is described at the end of this chapter. The possible values of the flag and their meaning are 3: highest quality, 2: fair quality, 1: uncertain detection, 0: no quality information available, -1 – likely false positive detection.

Flag_PPI

is based on the L-value distance between the SSFAC boundary and the MIT minimum. Since this difference has a strong MLT-dependence, first this trend is removed. Then the de-trended difference is used to define Flag_PPI as described above.

$$\text{trend:} \quad dL_{MITxTEC-PPIxFAC} = -0.178 \cdot MLT^{*} + 0.14 \qquad \text{Eq. 4.4-1}$$

quantiles: QQ_PPI = [-inf, -0.95, -0.53, -0.22, 0.34, 0.64, 1.06, inf]

Flag_ROC

is based on the rate of change (ROC, i.e., change per orbit) of the L-value of the MIT minimum. The flag values are derived from the ROC values as described above. First the closest (in time) of the three preceding observation is used to define the ROC and then this flag (Flag_ROCa). Then in a similar way, a flag value corresponding to the change be-tween the current and the following orbit (Flag_ROCp) is calculated. The maximum of the two flag values (Flag_ROCa and Flag_ROCp) defines the value of Flag_ROC. Whenever this flag has a high value (3 or 2), it means that the consecutive observations support each other. In a dynamic situation, at sudden changes, this flag can be low. Hence this flag alone cannot be used to assess the overall quality of the MIT detection.

quantiles: QQ_ROC = [-inf, -1.00, -0.59, -0.25, 0.25, 0.50, 0.84, inf]

Flag_Ne

is based on the L-value distance between the MIT minima derived from TEC and LP observations. This difference slightly depends on L, thus first this trend is removed. Then the de-trended difference is used to define Flag_Ne as de-scribed above.

trend: $dL_{MITxTEC-MITxLP} = -0.007 \cdot MLT^{*} + 0.04$

quantiles: QQ_ Ne = [-inf, -0.77, -0.37, -0.13, 0.18, 0.35, 0.60, inf]

Eq. 4.4-2

Flag_Te

is based on the L-value distance between the MIT minima derived from TEC and the Te peak derived from LP observa-tions. This difference slightly depends on L, thus first this trend is removed. Then the de-trended difference is used to define Flag_Te as described above.

trend: $dL_{\ MITxTEC-MITxLP\ SETE} = -0.007 \cdot \mathrm{MLT}^{*} + 0.04$

quantiles: QQ_Te = [-inf, -0.77, -0.37, -0.13, 0.18, 0.35, 0.60, inf]

Eq. 4.4-3

Flag_AOB

depends on the mutual position of the AOB boundary and the MIT minimum (1: AOB is poleward of the MIT minimum, -1: otherwise).

Flag_SZA

is calculated from the solar zenith angle at the MIT minimum (3: SZA>110°; 2: 110≥SZA>100°, 1: 100≥SZA>90°; -1: SZA≤90°).

Flag_WSA

indicates if the detection is made in the region potentially affected by the Weddell-See ionisation Anomaly. 1: detection outside the risk region, -1: detection inside the risk region. The region potentially affected by the WSA is de-fined with the following parameters: QD_Longitude is between 10° W and 150° W, QD_Longitude is between 30° S and 55° S, and day of the year is ≤90 or ≥305.

4.4.1 Flag_MIT

Now we return to the definition of the main quality flag that assesses the overall quality of the product record. Whenever Flag_WSA = -1 OR TEC<-1 then Flag_MIT = -1, i.e., in the Weddell-See Anomaly region, as well as when the MIT minimum is below -1 TECU the flag equals -1:

Flag_MIT = Flag_WSA (= -1).

If Flag_PPI=-1 OR L_MIT is EW of L_AOB-2 OR L_MIT>10 OR 10<MLT<14, then the detection is considered very low quality and removed from the product (close-to-noon observations at extremely high-L or well EW of AOB or far from the SSFAC boundary). Here, and in the following, L_MIT and L_AOB stand for L_Value of MITx_LP, and L_Value of AOBxFAC, respectively.

When no information of SSFAC boundary is available (Flag_PPI=0), the dayside observations cannot be verified. The risk increases with decreasing SZA and approaching MLT noon.

If Flag_PPI=0 AND (L_MIT<3 OR L_MIT>6 OR 6<MLT<18) AND SZA<100°, then the detection is considered very low quality and removed from the product (dayside observations at rather high or low L).

If Flag_PPI=0 AND (L_MIT<3 OR L_MIT>6 OR 6<MLT<18) AND SZA>=100°, then the detection is considered uncertain, hence

Flag_MIT = -1.

If Flag_PPI=0 AND 3<=L_MIT<=6 AND (MLT<=6 OR 18<=MLT), then Flag_MIT is estimated from Flag_ROC:

Flag_MIT = Flag_ROC-1.

When Flag_PPI>0 (MIT and the SSFAC boundary are at moderate distance) and Flag_ROC is defined (i.e., in most of the MIT detections), then these Flag_MIT mostly depends on these two flags.

If Flag_PPI>0 AND Flag_ROC>=0, then

Flag_MIT = max(Flag_PPI, Flag_ROC).

If Flag_PPI>0 AND Flag_ROC=-1, then

Flag_MIT = Flag_PPI – 1.

In the following, based on further considerations, Flag_MIT is further refined. Flag_Te and Flag_TEC are used to strengthen (increase) an already positive main flag if the SETE and TEC-based MIT observations confirm the LP-based MIT detection (i.e., they lie close to each other).

If Flag_MIT>0 AND max(Flag_Te,Flag_TEC)>Flag_MIT, then

Flag_MIT = Flag_MIT + 1.

The less certain detections (Flag_MIT<3) are further checked. These observations may be qualified questionable if they were made at very low or very high L. In other words, for the extreme cases, only the highest quality detections have positive main flag.

If {1<=Flag_MIT<=2 AND (L_MIT<2 OR 8<L_MIT<=10)} OR {0<=Flag_MIT<=1 AND (2<=L_MIT<3 OR 6<L_MIT<=8)}, then

Flag_MIT = -1.

If 0<=Flag_MIT<=1 AND (L_MIT<2 OR 8<L_MIT<=10), then the detection is considered poor quality and removed from the product.

4.4.2 Position_Quality_IDs

Position_Quality_ID is a vector of four elements corresponding to the four boundary positions defined for each MIT observations. The four positions are: 1 – TEC MIT EW edge of the EW wall ‘ee’; 2 – TEC MIT PW edge of the EW wall ‘ep’; 3 – TEC MIT EW edge of PW wall ‘pe’; and 4 – TEC MIT PW edge of the PW wall ‘pp’. The corresponding quality flags are depicted as follows:

Position_Quality_ID = [Flag_MIT_ee, Flag_MIT_ep, Flag_MIT_pe, Flag_MIT_pp],

where

Flag_MIT_ee [*Position_Quality_1*]

First, *Q* is calculated as

Q = 100*gradgrad_TEC_ee*mean(NS*grad_TEC)_ew/mean(TEC)_ew,

where xxx_ee is the value of xxx at the EW edge of the EW wall, mean()_ew stands for the interval mean taken within the EW wall. *Q*s less than 1/8 are all set to 1/16, *Q*s > 1 are all set to 1. Then Flag_MIT_ee is calculated as

Flag_MIT_ee = 3 + fix(log2(*Q*));

This gives a value between 1 and 3 for *Q* > 1/8, and -1 otherwise. A larger value corresponds to a steeper wall and a sharper contrast in steepness at the outer edge of the wall.

Flag_MIT_ep [*Position_Quality_2*]

First, *Q* is calculated as

Q = mean(NS*grad_TEC)_ew/ min(NS*grad_TEC)_ew,

where min()_ew stands for the interval minimum taken within the EW wall. *Q*s are treated the same way as above to derive the quality flag

Flag_MIT_ep = 3 + fix(log2(*Q*));

This gives a value between 1 and 3 for *Q* > 1/8, and -1 otherwise. A larger value corresponds to less structured (more linear) wall.

Flag_MIT_pe [*Position_Quality_3*]

If L_value_3 > 11 then Flag_MIT_pe = -1.

Otherwise, first, *Q* is calculated as

Q = mean(NS*grad_TEC)_pw/ max(NS*grad_TEC)_pw,

where max()_pw stands for the interval maximum taken within the PW wall. *Q*s are treated the same way as above to derive the quality flag

Flag_MIT_pe = 3 + fix(log2(*Q*));

This gives a value between 1 and 3 for *Q* > 1/8, and -1 otherwise. A larger value corresponds to less structured (more linear) wall.

Flag_MIT_pp [*Position_Quality_4*]

If L_value_4 > 14 then Flag_MIT_pp = -1.

Otherwise, first, *Q* is calculated as

Q = -100*gradgrad_TEC_pp*mean(NS*grad_TEC)_pw/mean(TEC)_pw,

where xxx_pp is the value of xxx at the PW edge of the PW wall, mean()_pw stands for the interval mean taken within the PW wall. *Q*s are treated the same way as above to derive the quality flag

Flag_MIT_pp = 3 + fix(log2(*Q*));

This gives a value between 1 and 3 for *Q* > 1/8, and -1 otherwise. A larger value corresponds to a steeper wall and a sharper contrast in steepness at the outer edge of the wall.

4.5 SSFAC boundary detection and the derivation of the midnight PP index

In this section, we summarise the main steps of data processing applied to Swarm observations to detect the SSFAC boundaries. The summary is based on [RD-1] and [RD-2].

4.5.1 Reading the data

Input data (FACxTMS L2 product) for the day considered are read from the source cdf file (Swarm native format). The daily data are complemented by the first segment fragment of the consecutive day, so that the daily data contains complete pole-to-pole orbits. At the same time, the first orbit fragment is dropped, since it is analysed together with data of the previous day. The orbit counter is read from the AUXxORBCNT product files.

4.5.2 Main steps of the detection process

For information on the calculation of magnetic coordinates, MLT, the L-value and solar zenith angles, see section 4.1.2.1.

4.5.2.1 *Segmentation of the data into quarter of orbits*

The same as described in section 4.1.2.2.

4.5.2.2 *Interpolating missing and flagged values*

No interpolation is applied for missing SSFAC values.

4.5.2.3 *De-noising*

No special de-noising is applied.

4.5.2.4 *Filtering, derivation of SSFACs*

First, the field-aligned current (FAC) density $j_{\parallel}$ (Level 2 product FACxTMS_2F) is high-pass filtered by a third-order Butterworth with a -3 dB cut-off at 250 mHz. The chosen high cut-off frequency ensuring precise boundary localization corresponds to a ~30 km spatial resolution along the (quasi-meridional) orbit. The resulting time series is what we call small-scale field aligned currents (SSFACs).

4.5.2.5 *Derivation of the SSFAC power level, i.e., the signal used for detection*

To derive the SSFAC power level S, what we call the detection signal, the logarithm of the squared SSFAC density (in units μA/m^2) is taken. Finally, the time series is boxcar averaged using a 20 s window length, i.e.

$$S = \langle \log_{10} j_{\parallel}^2 \rangle_{20\,\mathrm{s}}$$

We note, that the same signal is used by AEBS project to derive the auroral boundaries (AOB) from SSFACs.

4.5.2.6 *The process of SSFAC boundary detection*

The detection of the SSFAC inner (EW) boundary is a multistep process (see Figure 4-6). First, all quarter orbit segments are scanned for the innermost transition of S between two pre-defined reference levels (an increase of the SSFAC power S from $S_c = -5.5$ to $S_m = -2.5$).

More precisely, first we determine the position Lc (the yellow arrow in Figure 4-7), i.e., the lowest L-value (> 1.5) where S surpasses −2.5:

More precisely, first we determine the position Lc (the yellow arrow in Figure 4-7), i.e., the lowest L-value (> 1.5) where S surpasses −2.5:

$$L_c = \min(L)\,, S(L) > -2.5 \text{ and } L > 1.5$$

Then L_m, the highest L-value below L_c where S is less than −5.5 is chosen (magenta arrow in Figure 4-7):

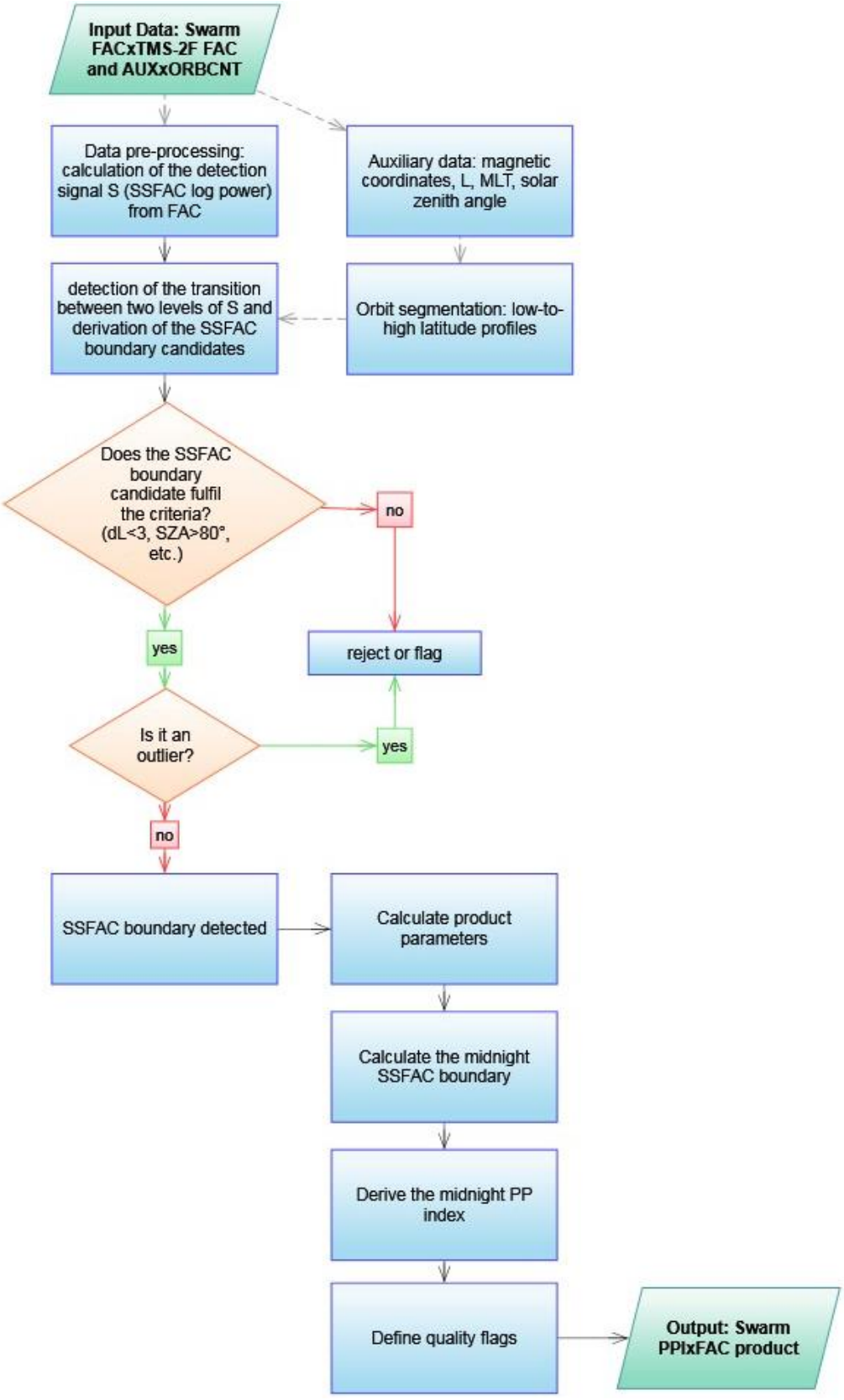

Figure 4-6 The process of detecting the SSFAC boundary and deriving the midnight PP index.

$$L_m = \max(L), S(L) < -5.5 \; and \; L < L_c.$$

The applied reference values are found typically only EW/PW of the ionospheric footprint of the nominal plasmapause. Their difference (= 3) means that the SSFAC power increases by a factor of 10^3.

In the next step, the change in the SSFAC power level within the transition zone $[L_c; L_m]$ is modelled by a linear fit, $S^* = aL + b$ (red dashed line in Figure 4-7), and σ, the RMS-value of the model residuals ($S - S^*$) in the $[L_c; L_m]$ interval is calculated.

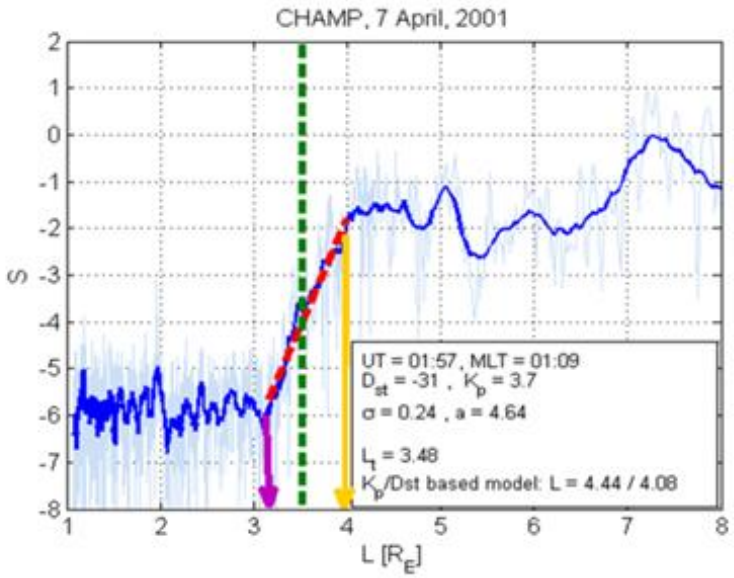

Figure 4-7 A well-defined boundary observed by CHAMP, the figure illustrates the main steps of the boundary detection.

The width of the boundary dL is then defined as $dL = L_c - L_m$. Finally, the L-value where S^* equals a third reference level, $S^*_{ref} = -4.1$, is taken as the position of the boundary, that is denoted by L_{ssfac} (the vertical green dashed line in Figure 4-7). Whenever L_{ssfac} lies outside the interval $[L_c; L_m]$, it is rejected. This typically happens when the boundary is poorly defined, mostly on the dayside. The fit quality parameters, dL (the boundary width) and σ (characterising the quality of the fit), are used to exclude less-defined transitions similarly as described in [RD-1].

Table 4-1 Reference levels of SSFAC power used for the detection of the SSFAC boundary.

	S_c	S^*_{ref}	S_m
CHAMP	-6.0	-3.8	-2.0
Swarm	-5.5	-4.0	-2.5

To optimize the quality of the detection results, a fine adjustment of the reference value S^*_{ref} based on maximizing the absolute correlation strength between the boundary position L_{ssfac} and the geomagnetic index Kp was performed (the final detection parameters are summarised in Table 4-1). This calibration was performed separately for CHAMP and Swarm observations ([RD-1] and [RD-2]). Allowing for comparisons on

shorter timescales than the 3 h cadence of Kp, the Kp index was linearly interpolated at UTs of the SSFAC index. During this and further calculations, Kp was delayed in time by 1 h. This time lag is inferred from a cross-correlation analysis between Kp and L_{ssfac}, and corresponds to the mean response time of the boundary to changes in geomagnetic activity.

4.5.3 Derivation of the SSFAC boundary model

In this section we discuss the derivation of the SSFAC boundary model based on [RD-2]. When plotted as a function of MLT on a dial plot, the mean boundary positions for a circle at any level of geomagnetic activity (see Figure 4-8, (a) the average position of the SSFAC boundary at different levels of geomagnetic activity as a function of MLT (all Swarm satellites), and (b) the MLT distribution of the SSFAC observations). This behaviour makes it possible to derive a simple boundary model that can be used to predict the boundary position for any MLT, Kp pair. The model is a circle with a Kp dependent radius and centre position.

The model (see Figure 4-9) can be formulated as

$$L_{mod} = c\cos d\varphi + \sqrt{R^2 - c^2\sin^2 d\varphi},$$

where $d\varphi = 2\pi\left(\frac{(MLT-MLT_c)}{24}\right)$ and $MLT_c = 24\ \cdot \varphi_c/360°$.

Moreover, we assume that both the position of centre of the circle C and the radius of the circle have a linear/quadratic dependence on Kp, respectively, that is

$$R = R_0 + p_1\mathrm{Kp} + p_2\mathrm{Kp}^2,$$

$$c = c_0 + \gamma_c\mathrm{Kp},$$

$$c = c_0 + \gamma_c\mathrm{Kp},$$

where c_0, MLT_0 define the centre and R_0 is the radius of the circle, both at Kp=0, while $p_1, p_2, \gamma_c, \gamma_{mlt}$ are free model parameters.

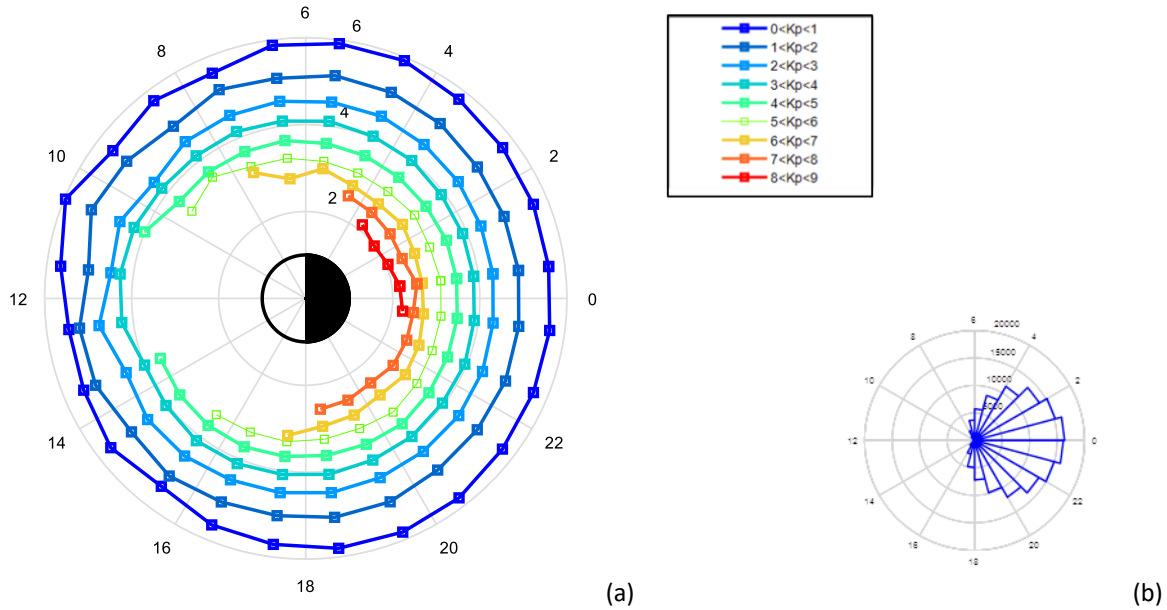

Figure 4-8 (a) the average position of the SSFAC boundary at different levels of geomagnetic activity as a function of MLT (all Swarm satellites), and (b) the MLT distribution of the SSFAC observations.

The parameters can be derived by fitting the model to all available observations. The resulting parameters (along with the 95% confidence intervals) are:

$$R_0 = 6.062 \pm 0.014\ R_E$$

$$p_1 = -0.6844 \pm 0.007\ R_E$$

$$p_2 = 0.03089 \pm 0.0009\ R_E$$

$$c_0 = 0.1539 \pm 0.015\ R_E$$

$$MLT_0 = 10.69 \pm 0.21\ \text{h}$$

$$\gamma_c = -0.00445 \pm 0.00435\ R_E$$

$$\gamma_{mlt} = 0.4018 \pm 0.061\ \text{h}.$$

This version of the model was built using CHAMP 2001-2008 and Swarm 2014-2019 observations (161 137 observations). The model will be up-dated as part of the validation work by the end of the project using all available CHAMP and Swarm boundary observations.

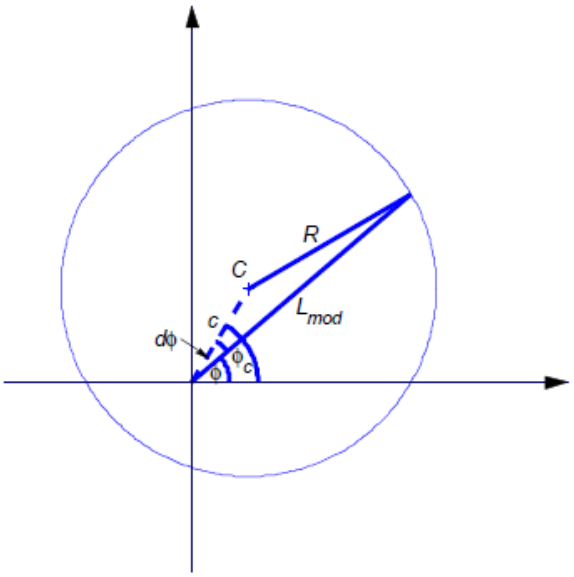

Figure 4-9 Illustration of the SSFAC boundary model parameters (not to scale).

4.5.4 Propagating a boundary observation made at some MLT to another MLT

When Kp is not known, that is a typical situation for real-time processing, one can start from the actual observed value and the MLT of the observation to calculate the boundary position at any other MLT. Having an observation of $L_{ssfac} = L_{obs}$ at a certain MLT_{obs}, we can, by combining the model (yielding the shape and the centre of the boundary) with the actual observation (providing the actual radius), estimate L_{ssfac} at any other MLT. This is done by rescaling the radius of the boundary based on the actual observation, while taking the average circular shape the centre position from the model:

$$R_{obs} = \sqrt{L_{obs}^2 + c^2 - 2cL_{obs}\cos d\varphi_{obs}}.$$

Since the Kp dependence of the centre position is found very weak [RD-2], it can be ignored and we can take them as constants ($c = 0.2\ R_E$ and $MLT_c = 12\ h$), while $d\varphi_{obs} = 2\pi(MLT_{obs} - MLT_c)/24$ can be calculated from the model. This simplification introduces less than 0.05 R_E error in the result. Now L_{mod} at any MLT can be computed by using:

$$L_{mod} = c\cos d\varphi + \sqrt{R_{obs}^2 - c^2 \sin^2 d\varphi}.$$

4.5.5 Derivation of the midnight PP index

We can use the above method, to calculate the SSFAC boundary position at midnight from any observations. The midnight position is important, because it was found by [RD-1] and [RD-2], that this is the region where the SSFAC boundary is the closest to the PP boundary, and where the dynamics of the two boundaries are coupled. For this particular case $d\varphi$ simplifies to π, and

$$L_{ssfac\_midnight} = R_{obs} - c.$$

This value could be called the midnight SSFAC index. Simultaneous PP observations (e.g., from Van Allen Probes or THEMIS) can be used to calibrate this proxy and to derive the correction term $\Delta L_{midnight}$ (a Kp or R_{obs} dependent constant) that will be used to calculate the midnight PP index as:

$$L_{PP\_midnight} = L_{ssfac\_midnight} + \Delta L_{midnight}.$$

Based on earlier work [RD-1], the typical value of $\Delta L_{midnight}$ is less than 0.3-0.5 R_E, and it decreases with increasing geomagnetic activity (higher Kp). The correction term will be updated by the end of this project as a result of the validation.

4.6 Definition of PPIxFAC_2F quality flags

The Quality parameter is a vector of eight flag values defined below in the order of their position in the Quality vector. The first of these is the main flag. For scientific case/statistical studies the use of data with main flag > 2/1 is recommended.

Flag_PPI

is the main flag characterising the overall quality of the product. It is derived from the other flags and other information. 3: highest quality, 2: fair quality, 1: uncertain detection, 0: no quality information available, -1: likely false positive detection).

Flag_ROC

is based on the rate of change (change per orbit) of the L-value of the SSFAC boundary. The flags 3, 2, and 1 are derived from the ROC the same way as for Flag_PPI, and in addition, ROC value below the 0.025 or above the 0.975 quantile is flagged by -1. To derive Flag_ROC, first the available closest of the three preceding observation is used to define a flag (Flag_ROCa). Then in a similar way, a flag corresponding to the change between the current and the following orbit (Flag_ROCp) is calculated. The maximum of the two (Flag_ROCa and Flag_ROCp) is taken as Flag_ROC.

quantiles: QQ_ROC = [-inf, -1.00, -0.59, -0.25, 0.25, 0.50, 0.84, inf]

Flag_Ne

is based on the L-value distance between the SSFAC boundary and MIT minimum derived from LP observations. Since this difference is highly depends on MLT, first, this linear trend is removed. The flag

thresholds are the [0 0.025 0.10 0.25 0.75 0.90 0.975 1] quantiles of the de-trended difference derived from statistics. The quantiles-defined intervals correspond to the -1, 1, 2, 3, 2, 1, -1 flag values, respectively.

trend: $dL_{PPIxFAC-MITxLP} = 0.178 \cdot MLT^* - 0.14$

quantiles: QQ_Ne = [-inf, -1.06, -0.64, -0.34, 0.22, 0.53, 0.95, inf] Eq. 4.6-1

Flag_Te

is based on the L-value distance between the SSFAC boundary and the MIT related Te peak derived from LP observations. The flag is derived the same way as Flag Ne.

trend: $dL_{PPIxFAC-MITxLP\ SETE} = 0.178 \cdot MLT^* - 0.06$

quantiles: QQ_Te = [-inf, -1.28, -.71, -0.35, 0.24, 0.58, 1.08, inf] Eq. 4.6-2

Flag_TEC

is based on the L-value distance between the SSFAC boundary and the MIT minimum derived from GPS TEC observations. The flag is derived the same way as Flag Ne.

trend: $dL_{PPIxFAC-MITxTEC} = 0.135 \cdot MLT^* - 0.00$

quantiles: QQ_TEC = [-inf, -0.99, -0.57, -0.29, 0.24, 0.56, 0.93, inf] Eq. 4.6-3

Flag_AOB

depends on the mutual position of the AOB boundary and the SSFAC boundary (1: AOB is poleward of the MIT minimum, -1: otherwise).

Flag_SZA

is calculated from the solar zenith angle at the SSFAC boundary (3: SZA>110°; 2: 110≥SZA>100°, 1: 100≥SZA>90°; -1: SZA≤90°).

Flag_WSA

indicates if the detection is made in the region potentially affected by the Weddel-See ionisation Anomaly. 1: detection outside the risk region, -1: detection inside the risk region. The region potentially affected by the WSA is defined with the following parameters: QD_Longitude is between 10° W and 150° W, QD_Longitude is between 30° S and 55° S, and day of the year is ≤90 or ≥305.

4.6.1 Position_Quality_IDs

Position_Quality_ID is a vector of two elements corresponding to the edge positions defined for each SSFAC boundary observations. The two positions are: 1 – EW edge of the SSFAC transition zone ‘ew’; 2 – PW edge of the SSFAC transition zone ‘pw’. The corresponding quality flags are depicted as follows:

Position_Quality_ID = [Flag_PPI_ew, Flag_PPI_pw],

where

Flag_PPI_ew

Flag_PPI_ew is based on the parameter σ that in turn depends on how well a linear can be fitted to the values in the transition zone where the SSFAC values increase orders of magnitudes. The lower the σ, the better the fit is.

Flag_PPI_ew = 3 if $\sigma < 0.25$,

Flag_PPI_ew = 2 if $0.25 \leq \sigma < 0.50$,

Flag_PPI_ew = 1 if $0.50 \leq \sigma$ and Flag_PPI_SZA(1) > 0,

Flag_PPI_ew = -1 if $0.50 \leq \sigma$ and Flag_PPI_SZA(1) = -1.

Flag_PPI_pw

Flag_PPI_pw is calculated in a similar way but the SZA at the PW position is used instead of the SZA at the EW position.

Flag_PPI_pw = 3 if $\sigma < 0.25$,

Flag_PPI_pw = 2 if $0.25 \leq \sigma < 0.50$,

Flag_PPI_pw = 1 if $0.50 \leq \sigma$ and Flag_PPI_SZA(2) > 0,

Flag_PPI_pw = -1 if $0.50 \leq \sigma$ and Flag_PPI_SZA(2) = -1.

5 Summary

This document discusses the derivation of the three PRISM products **MITx_LP_2F** (section 4.1), **MITxTEC_2F** (section 4.3) and **PPIxFAC_2F** (section 4.5) in detail and also the background knowledge the products and their derivations are based on. The description of the definition of the corresponding quality flags are given in sections 4.2, 4.4 and 4.6 and for MITx_LP_2F, MITxTEC_2F and PPIxFAC_2F, respectively.